

Mathematical modeling of the influence of RKIP on the ERK signaling pathway

Kwang-Hyun Cho^{1*}, Sung-Young Shin¹, Hyun-Woo Kim¹, Olaf Wolkenhauer^{2*}, Brian McFerran^{3,4} and Walter Kolch^{3,5}

¹ School of Electrical Engineering, University of Ulsan
Ulsan, 680-749, Korea

{ckh, syshin, hwkim}@mail.ulsan.ac.kr

² Dept. of Biomolecular Sciences and Dept. of Electrical Engineering and Electronics
UMIST, Manchester, M60 1QD, U.K.

olaf.wolkenhauer@umist.ac.uk

³ Beatson Institute for Cancer Research, Cancer Research UK Beatson Laboratories
Switchback Road, Bearsdn, Glasgow, G61 1BD, U.K.

wkolch@beatson.gla.ac.uk

⁴ Organon Laboratories, Newhouse, Motherwell, U.K.

B.McFerran@organon.co.uk

⁵ Institute of Biomedical and Life Sciences, University of Glasgow, University Avenue,
Glasgow, G12 8QQ, U.K.

Abstract. This paper investigates the influence of the Raf Kinase Inhibitor Protein (RKIP) on the Extracellular signal Regulated Kinase (ERK) signaling pathway through mathematical modeling and simulation. Using nonlinear ordinary differential equations to represent biochemical reactions in the pathway, we suggest a technique for parameter estimation, utilizing time series data of proteins involved in the signaling pathway. The mathematical model allows the simulation the sensitivity of the ERK pathway to variations of initial RKIP and ERK-PP (phosphorylated ERK) concentrations along with time. Throughout the simulation study, we can qualitatively validate the proposed mathematical model compared with experimental results.

1 Introduction

The Ras/Raf-1/MEK/ERK module is a ubiquitously expressed signaling pathway that conveys mitogenic and differentiation signals from the cell membrane to the nucleus. This kinase cascade appears to be spatially organized in a signaling complex nucleated by Ras proteins. The small G protein Ras is activated by many growth factor receptors and binds to the Raf-1 kinase with high affinity when activated. This induces the recruitment of Raf-1 from the cytosol to the cell membrane. Activated Raf-

*Corresponding authors.

It then phosphorylates and activates MAPK/ERK Kinase (MEK), a kinase that in turn phosphorylates and activates Extracellular signal Regulated Kinase (ERK), the prototypic Mitogen-Activated Protein Kinase (MAPK). Activated ERKs can translocate to the nucleus and regulate gene expression by the phosphorylation of transcription factors [1]. This kinase cascade controls the proliferation and differentiation of different cell types. The specific biological effects are crucially dependent on the amplitude and kinetics of ERK activity [7]. The adjustment of these parameters involves the regulation of protein interactions within this pathway. Here the Raf-1 kinase inhibitor protein (RKIP) plays a central role. RKIP binds to Raf-1 and MEK thereby disrupting the interaction between Raf-1 and MEK. As a consequence RKIP inhibits the phosphorylation and activation of MEK by Raf-1. RKIP overexpression interferes with the activation of MEK and ERK, induction of AP-1-dependent reporter genes and transformation elicited by an oncogenically activated Raf-1 kinase. Downregulation of endogenous RKIP by expression of antisense RNA or antibody microinjection induces the activation of MEK-, ERK-, AP-1-dependent transcription. Thus, RKIP represents a new class of protein-kinase-inhibitor protein that regulates the activity of the Raf-1/MEK/ERK module [2].

In this paper we are using an integrated approach of mathematical modeling in combination with experimental data to investigate the impact of RKIP on the dynamics of the ERK pathway. For this purpose, we establish a mathematical model of the signaling pathway consisting of a set of nonlinear ordinary differential equations (ODEs) to represent enzyme kinetic reactions. To complete and to simulate this mathematical model, we need to identify (or estimate) all the parameter occurring in these equations. Parameter estimation for nonlinear differential equations is non-trivial and provides a major challenge in modeling signaling pathways.

One could argue that parameter estimation is currently the limiting step in biomathematical modeling [3], [4], [6]. In order to tackle this problem, we propose a simple method for parameter estimation utilizing time course measured data. This method first discretizes the nonlinear ODEs into algebraic difference equations that are linear with respect to the parameters and then solve the transformed linear algebraic difference equations to obtain the parameter values at each frozen time point. We can then obtain the required parameter values using regression techniques. Based on the estimated parameter values, we perform a sensitivity analysis of the ERK pathway in order to discuss the influence of RKIP through simulation. The simulation study reveals the sensitivity of all the protein concentration involved in the pathway with respect to the variation of initial RKIP and phosphorylated ERK (ERK-PP) concentrations in a quantitative manner.

The paper is organized as follows. Section 2 briefly introduces the new parameter estimation method for mathematical modeling. Section 3 describes the ERK signaling pathway and its suppression by RKIP. Section 4 shows the parameter estimation of the ERK signaling pathway suppressed by RKIP and the simulation results. Finally, conclusions and further studies are found in Section 5. The detailed mathematical model of the ERK signaling pathway suppressed by RKIP, time course data, and estimated parameter values are summarized in Appendix.

2 Parameter estimation based on time course data

In this section we discuss the topic of parameter estimation and exemplify it via the ERK signaling pathway suppressed by RKIP as illustrated in Fig. 1. To estimate parameter values of nonlinear ODEs, we first discretize the given continuous differential equations along with a sample time, which usually corresponds to the time of measurement. Then the continuous differential equations can be approximated by difference equations. Consider the following continuous nonlinear ODEs in (1).

$$\begin{aligned}\frac{dx_1}{dt} &= f_1(x_1, x_2, \dots, x_m; k_1, k_2, \dots, k_m) \\ \frac{dx_2}{dt} &= f_2(x_1, x_2, \dots, x_m; k_1, k_2, \dots, k_m) \\ &\vdots \\ \frac{dx_m}{dt} &= f_m(x_1, x_2, \dots, x_m; k_1, k_2, \dots, k_m)\end{aligned}\quad (1)$$

We can approximate the differential operator by a difference operator for small sampling time interval as follows.

$$\left. \frac{dx_i(t_n)}{dt} \cong \frac{x_i(t_n) - x_i(t_{n-1})}{t_n - t_{n-1}} \right|_{i=1,2,\dots,m} \quad (2)$$

Note that this is only a first order approximation and we can alternatively employ any other kind of approximation to reduce the approximation error.

$$\begin{aligned}\frac{x_1(t_n) - x_1(t_{n-1})}{t_n - t_{n-1}} &\cong f_1(x_1(t_n), x_2(t_n), \dots, x_m(t_n); k_1(t_n), k_2(t_n), \dots, k_m(t_n)) \\ \frac{x_2(t_n) - x_2(t_{n-1})}{t_n - t_{n-1}} &\cong f_2(x_1(t_n), x_2(t_n), \dots, x_m(t_n); k_1(t_n), k_2(t_n), \dots, k_m(t_n)) \\ &\vdots \\ \frac{x_m(t_n) - x_m(t_{n-1})}{t_n - t_{n-1}} &\cong f_m(x_1(t_n), x_2(t_n), \dots, x_m(t_n); k_1(t_n), k_2(t_n), \dots, k_m(t_n))\end{aligned}\quad (3)$$

In most of cases when we derive eq. (1) based on enzyme kinetics, (3) becomes a set of linear algebraic difference equations with respect to parameters $k_i(t_n)|_{i=1,2,\dots,m}$ for each frozen time point t_n . Hence we can obtain the following set of estimated parameter values by solving such linear algebraic simultaneous difference equations.

$$\begin{aligned}k_1(t_n) &\cong g_1(x_1(t_n), x_2(t_n), \dots, x_m(t_{n-1}), x_1(t_{n-1}), x_2(t_{n-1}), \dots, x_m(t_{n-1})) \\ k_2(t_n) &\cong g_2(x_1(t_n), x_2(t_n), \dots, x_m(t_{n-1}), x_1(t_{n-1}), x_2(t_{n-1}), \dots, x_m(t_{n-1})) \\ &\vdots \\ k_m(t_n) &\cong g_m(x_1(t_n), x_2(t_n), \dots, x_m(t_{n-1}), x_1(t_{n-1}), x_2(t_{n-1}), \dots, x_m(t_{n-1}))\end{aligned}\quad (4)$$

The resultant estimated parameter values $k_i(t_n)|_{i=1,2,\dots,m}$ might include time dependent experimental noise components which can be further eliminated by regression techniques. After all, if the system itself is time-independent then these time series of $k_i(t_n)|_{i=1,2,\dots,m}$ will converge to certain steady-state values. Otherwise it can be approximated by interpolation of polynomial functions. This approach has two advantages: 1) it is applicable to not only time-invariant systems (estimation of constant parameter values) but also time-varying systems (estimation of a parameter function of time), 2) the estimation error can be reduced by decreasing the sampling time interval. On the other hand it is disadvantageous in that it requires multiple measurements for time course data of each protein involved in the signaling pathway and is therefore unlikely to be popular with the experimentalists. However, this does not impair the proposed method since we can transform commonly used WB (western blotting) data into the required concentration data under reasonable assumptions.

3 ERK signaling pathway regulated by RKIP

This section illustrates the foregoing parameter estimation method using a mathematical model of the ERK signaling pathway regulated by RKIP. Consider first a graphical representation of the signaling pathway shown in Fig. 1 where m_1 denotes the concentration of the activated Raf-1 (also denoted as Raf-1*), m_2 denotes the concentration of RKIP, m_3 denotes the concentration of Raf-1*/RKIP complex, and so on. In fact, Fig. 1 illustrates only part of the ERK pathway, i.e. it considers the subset of the ERK pathway regulated by RKIP. In the remainder of this paper we confine our discussion on parameter estimation to this pathway. Figure 1 describes the following consecutive mechanisms: 1) RKIP inhibits Raf-1* to phosphorylate MEK by binding to Raf-1* and forming a complex Raf-1*/RKIP, 2) Free Raf-1* phosphorylates MEK and converts inactive MEK into active MEK-PP. MEK-PP binds to ERK and phosphorylates it to active ERK-PP. ERK-PP can interact with the Raf-1*/RKIP complex to form a Raf-1*/RKIP/ERK-PP complex, 3) Then ERK-PP phosphorylates RKIP into RKIP-P causing the release of Raf-1* from RKIP-P. ERK does not dephosphorylate itself. ERK is dephosphorylated by Protein Phosphatase 2A (PP2A) and MAPK Phosphatases, MKPs [8]. The expression of MKP-1 is transcriptionally induced by ERK. In contrast, MKP-3 is constitutively expressed, but binding of ERK enhances its phosphatase activity. MKP-3 seems to serve as an anchor protein which binds ERK in resting cells keeping it inactive. PP2A is a constitutively expressed and constitutively active phosphatases, which probably is regulated by selective targeting to its substrates, 4) Raf-1* returns to its original active state Raf-1* after being released from the Raf-1*/RKIP-P/ERK-PP complex, 5) The timecourse analysis of ERK-PP and Raf-1*/RKIP complex formation rather suggest the following: The increase in free Raf-1* causes a further increase of MEK-PP and eventually ERK-PP, 6) The RKIP-phosphatase (RP) is artificially introduced to complete this model by

showing the dephosphorylation of RKIP-P into the original active state RKIP. After dephosphorylation RKIP binds to Raf-1* and suppresses further phosphorylation and activation of MEK. MEK-PP and ERK-PP levels rapidly decline due to efficient dephosphorylation by PP2A and MKPs.

Based on enzyme kinetics, we can derive a mathematical model, a set of nonlinear ODEs of this signaling pathway with respect to state variables $m_i \Big|_{i=1,2,\dots,11}$ as shown by (5) in Appendix. For the purpose of simulation of this mathematical model, the initial value of all complex proteins and product proteins are assumed to be zero and other initial values such as signaling proteins, $m_1, m_2, m_7, m_9, m_{10}$ are defined according to measured time course data. Based on the time course data, found in Table 2 and 3 of the Appendix, we can apply the proposed parameter estimation to this model, which is explained in detail in next section. The resultant parameter time series are also summarized in Table 4 and 5 of the Appendix.

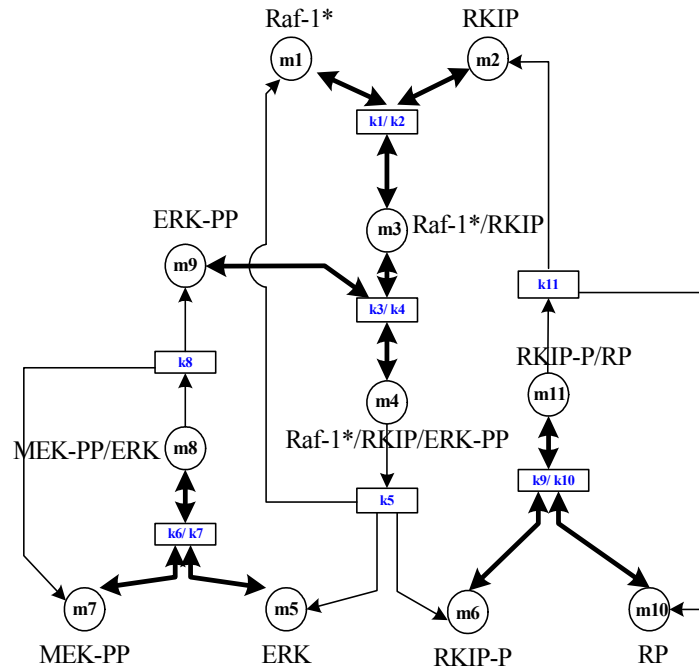


Fig. 1. Graphical representation of the ERK signaling pathway Regulated by RKIP: a circle \bigcirc represents a state for the concentration of a protein and a bar \square a kinetic parameter of reaction to be estimated. The directed arc (arrows) connecting a circle and a bar represents a direction of a signal flow. The bi-directional thick arrows represent an association and a dissociation rate at same time. The thin unidirectional arrows represent a production rate of products.

4. Parameter estimation and simulation studies

4.1 Parameter estimation

The estimated parameters usually appear as a time dependent profile since the time course data include various uncertain factors such as transient responses, noise terms, etc. However, if the signal transduction system itself is inherently time-invariant then estimated parameter profile should converge to a certain constant value at steady-state. Therefore we have to find this convergence value if the system is time-invariant. Otherwise we have to derive an interpolated polynomial function of time for time-varying systems.

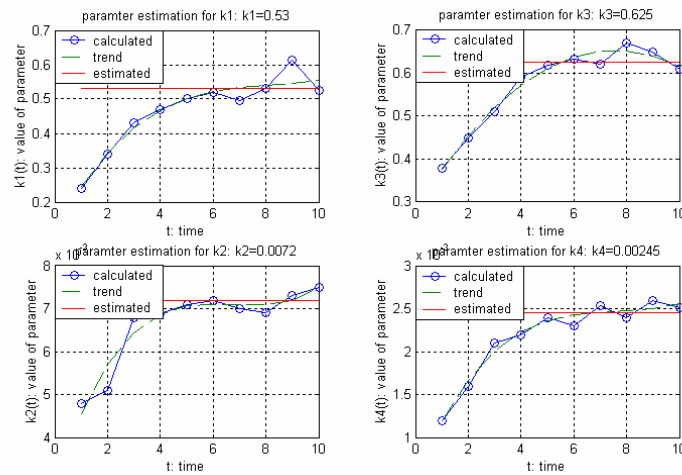


Fig. 2. Parameter estimation process from time series data: the upper left shows Raf-1*/RKIP complex association parameter k_1 , the upper right shows Raf-1*/RKIP/ERK-PP association parameter k_3 , the lower left shows Raf-1* and RKIP dissociation parameter k_2 , and the lower right shows ERK-PP and Raf-1*/RKIP complex dissociation parameter k_4 .

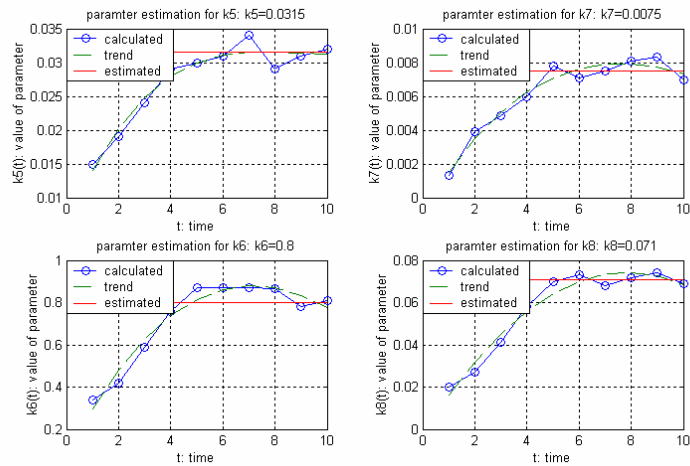


Fig. 3. Parameter estimation (cont'd): the upper left shows Raf-1*, ERK-P, and RKIP-P production parameter k_5 , the upper right shows MEK-PP and ERK dissociation parameter k_7 , the lower left shows MEK-PP/ERK association parameter k_6 , and the lower right shows ERK-PP production parameter k_8 . James O'Ferrell's data from frog oocytes that ERK phosphorylation is non-processive, ie proceeds ERK->ERK-P->ERK-PP, may not apply in mammalian cells. We looked in NIH cells and did not see it. Therefore, and for the sake of simplicity we can simply assume that the reaction catalysed by MEK is ERK->ERK-PP.

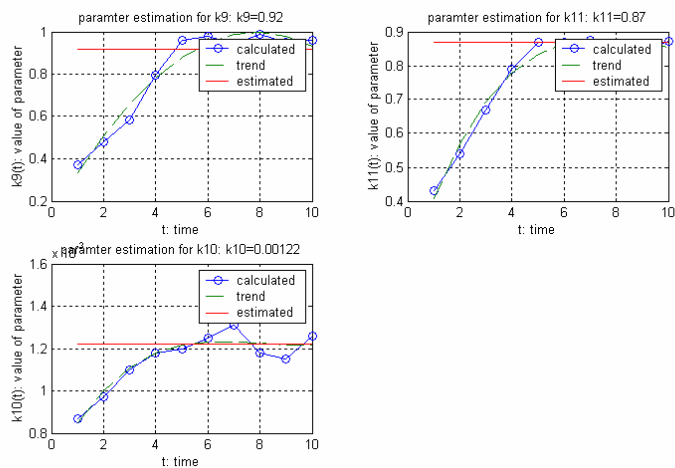


Fig. 4. Parameter estimation process upon the time course data: the upper left shows RKIP-P/RP association parameter k_9 , the upper right shows RKIP and RP production parameter k_7 , and the lower left shows RKIP-P and RP dissociation parameter k_{10} .

Figures 2 to 4 show the process of parameter estimation from the time series. Estimated parameter values can be found as the convergence point since the parameter profile shows time-invariant characteristics. In each plot, we calculate the converging parameter value and the resultant estimation as summarized in Table 1. These estimated parameter values are used for the simulation studies in the following sections.

Table 1. Summary of the estimated parameter values.

Parameter	Estimated Value	Parameter	Estimated Value	Parameter	Estimated Value	Parameter	Estimated Value
k1	0.53	k2	0.0072	k3	0.625	k4	0.00245
k5	0.0315	k6	0.8	k7	0.0075	k8	0.071
k9	0.92	k10	0.00122	k11	0.87		

4.2 Two-dimensional simulation for fixed initial conditions

Based on the mathematical model summarized in Appendix and the estimated parameter values in Table 1, we perform simulation studies to analyze the signal transduction system with respect to the sensitivity for the variation of RKIP and ERK-PP. For this purpose, we first simulate the pathway model according to the variation of the initial concentration of RKIP (RKIP sensitivity analysis). Next we perform the simulation according to the variation of the initial concentration of ERK-PP in this case (ERK-PP sensitivity analysis). Since ERK-PP causes the release of Raf-1* from the Raf-1*/RKIP/ERK-PP complex, the inhibitory effect of RKIP is dependent upon the concentration of ERK-PP and therefore this ERK-PP sensitivity analysis is very important to understand the ERK pathway suppressed by RKIP.

Figure 5 shows the simulation results for fixed initial conditions. The upper left of Fig. 5 shows the dynamics of Raf-1*, RKIP, and Raf-1*/RKIP complex. We can see Raf-1* quickly binds to RKIP, but after a while Raf-1* and RKIP reach their steady states. The upper right shows the activity of MEK-PP which phosphorylates ERK. The concentration of ERK-P/MEK-PP complex increases up to about 0.5 μM . Although it is not shown here, this complex concentration however might decrease after a while since the phosphorylated ERK-P (ERK-PP) is released from the complex. The lower left shows the activity of ERK-PP which phosphorylates RKIP in the Raf-1*/RKIP complex and then also releases Raf-1* from the complex. We can see that Raf-1*/RKIP complex also decreases to a steady state. The lower right shows the activity of the RKIP Phosphatase (RP). In this case, it changes very little; however, for different initial conditions corresponding to different microenvironments such as different *in-vivo* conditions it could change dramatically. After all, throughout these simulation results, we can confirm the crucial role of RKIP as an inhibitor of the ERK pathway by binding to Raf-1* and dissociating the Raf-1*/MEK complex. Our simulation allows us to now make quantitative predictions of the impact of RKIP on the activity of the ERK pathway in different cells lines and at different conditions of stimulation.

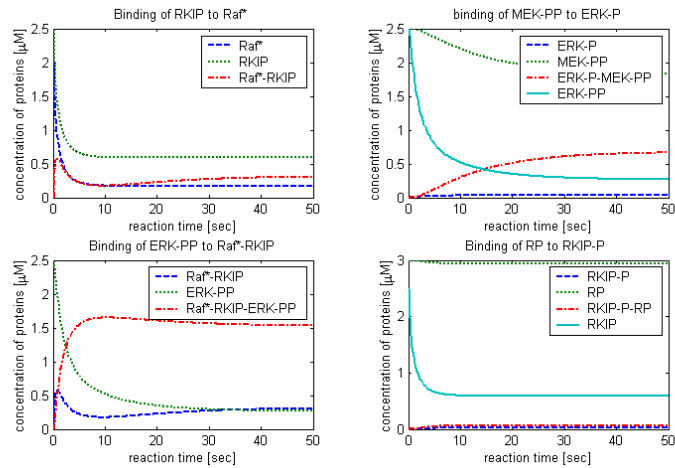


Fig. 5. Simulation results of the mathematical modeling for fixed initial condition: the upper left shows the dynamics for Raf-1*, RKIP, and their complex Raf-1*/RKIP, the upper right shows the activity of MEK-PP which phosphorylates and activates ERK, the lower left shows the activity of ERK-PP, and the lower right shows the activity of RP.

4.3 Sensitivity analysis according to the variation of initial RKIP

In this section, we show the sensitivity analysis with respect to the variation of initial RKIP. RKIP has been recently identified as a potent Raf-1* inhibitor in the ERK pathway. RKIP binds to Raf-1* and thereby prevents Raf-1* from phosphorylating and activating MEK. Based on the variation of the concentration of RKIP from 0.5 to 5 μM , we investigate its effect to the concentration change of other proteins. We find that if the initial concentration of RKIP increases over time then the concentration of active MEK-PP and ERK-PP decreases while the concentrations of inactive MEK and ERK increase at the same time. Likewise, when the concentration of RKIP increases linearly along with time, the concentration of Raf-1* available to activate MEK decreases exponentially. Under these conditions RKIP-P increases exponentially, because more RKIP is available for phosphorylation by ERK-PP, and ERK-PP does not immediately decline when MEK activation is inhibited. Eventually, as ERK-PP is being dephosphorylated, the levels of MEK and RKIP-P reach steady-state values. Likewise MEK-PP decreases to steady-state level. If all Raf-1* becomes engaged by RKIP then the ERK pathway becomes completely suppressed since no MEK-PP can be generated.

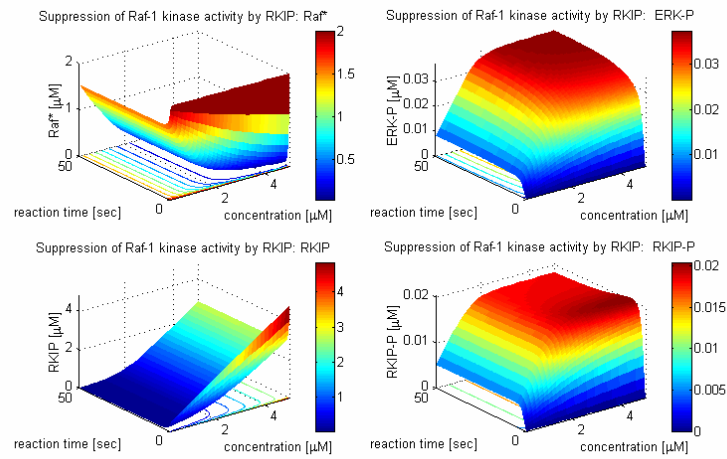


Fig. 6. The simulation results according to the variation of the concentration of RKIP: The upper left shows the change of concentration of Raf-1*, the upper right shows ERK, the lower left shows RKIP, and the lower right shows RKIP-P.

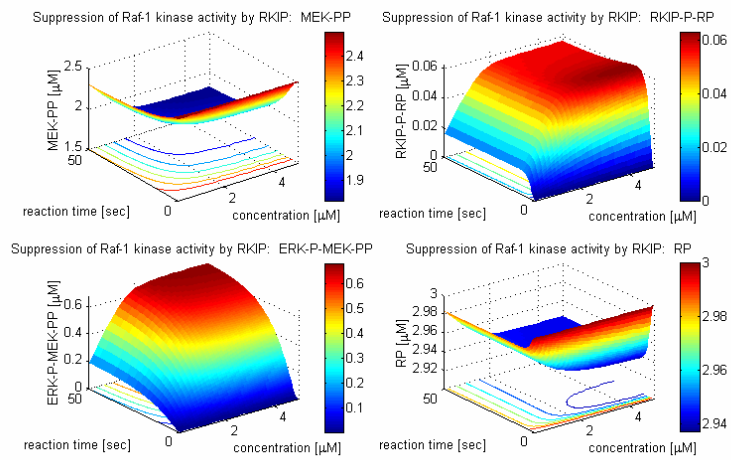


Fig. 7. The simulation results according to the variation of the concentration of RKIP (continued): The upper left shows the change of concentration of MEK-PP, the upper right shows RKIP-P-RP, the lower left shows ERK-P-MEK-PP, and the lower right shows RP.

4.4 Sensitivity analysis according to the variation of initial ERK-PP

In this section, we show the sensitivity analysis with respect to the variation of initial ERK-PP reflecting different basal activities of the ERK pathway in different cell

types. By changing the concentration of ERK-PP from 0.5 to 5 μM , we investigate the change of concentration for other proteins.

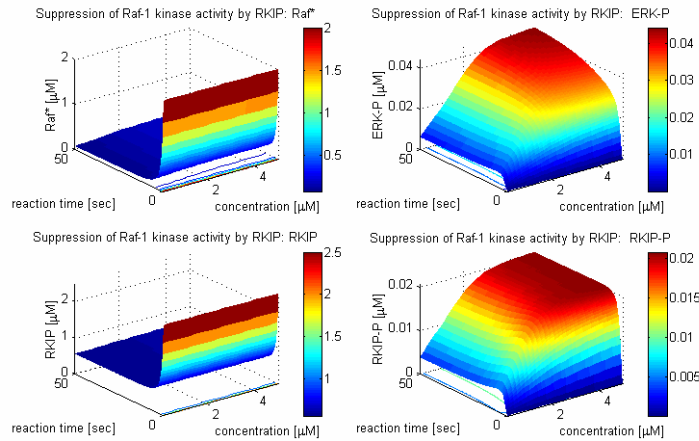


Fig. 8 The simulation results according to the variation of the concentration of ERK-PP: The upper left shows the change of concentration of Raf-1*, the upper right shows ERK-P, the lower left shows RKIP, and the lower right shows RKIP-P.

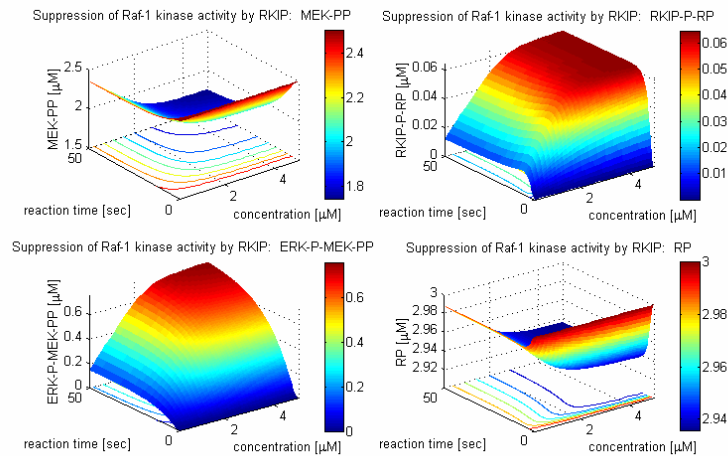


Fig. 9 The simulation results according to the variation of the concentration of ERK-PP (continued): The upper left shows the change of concentration of MEK-PP, the upper right shows RKIP-P-RP, the lower left shows ERK-P-MEK-PP, and the lower right shows RP.

5 Concluding remarks and further studies

In this paper, we introduced a system-theoretic approach to the analysis and quantitative modeling of the ERK pathway regulated by RKIP. To this end, a parameter estimation technique was proposed by first approximating the differential operator by a difference operator and then by utilizing time course data to resolve the transformed simultaneous linear algebraic difference equations with respect to parameters for each frozen time point. The estimated parameter time series show a profile converging to a constant value at steady-state, suggesting signal transduction system is time-invariant. For a simulation study of the ERK pathway regulated by RKIP, we made use of these parameter values in a model of nonlinear ODEs. Based on this mathematical model, we performed the sensitivity analysis of the pathway with respect to the initial RKIP and ERK-PP variation. These simulation studies provide a qualitative validation of the mathematical model compared to experimental results in view of the transient behavior and sensitivity analysis.

A remarkable result of this simulation is that RKIP inhibition of the Raf-MEK-ERK pathway is non-linear. This is completely unexpected given that RKIP acts as a stoichiometric inhibitor, which in enzyme kinetic assays behaves like a competitor for substrate, i.e. MEK [1]. The non-linearity appears to be caused by a previously unaccounted feedback phosphorylation of RKIP induced through the ERK pathway. This phosphorylation diminishes the affinity of RKIP for Raf-1 [McFerran et al., manuscript in preparation]. As Fig. 6 shows the maximal sequestration of Raf-1 by RKIP occurs at a particular RKIP expression level. However, the prevention of MEK-PP accumulation is mainly a function of time. The expression level of RKIP determines the kinetics of MEK-PP decrease rather than the final extent (Fig. 7). At the level of ERK activation this translates into a response curve with a steep initial slope, but very different levels of final activity (Fig. 7). Importantly, this predicted behavior correlates with experimental data that revealed a non-linearity of RKIP inhibition of the Raf-MEK-ERK pathway [2]. In these experiments RKIP mediated inhibition reached a saturation level rather than showing a linear decline. Our simulation model confirms and explains this experimentally determined behavior of the pathway. It also makes a further important prediction, namely that RKIP modulates the final extent and duration of ERK activity rather than the initial activation kinetics. This property assigns RKIP a crucial role as a decision maker in situations where the level and duration of ERK activity determines the biological outcome. It will be interesting to test this prediction in a relevant biological system such as PC12 cell. The proliferation of these cells is stimulated by a short burst of ERK activity, whereas differentiation requires a sustained level of high ERK activity. Our simulation model would predict that RKIP will preferentially interfere with differentiation and would redirect the biological decision to a proliferation response.

In order to further investigate the influence of RKIP on the ERK signaling pathway, we wish to expand on the proposed mathematical modeling and simulation studies to cover more aspects of the ERK pathway. This will involve time consuming experiments to allow parameter identification from time series data. However, we deem it necessary to develop simulation models hand in hand with experimental validation. The current study shows that simulation actually can aid in the interpretation of ex-

perimental data and promote the formulation of new hypotheses that provide direction in the investigation of complex biological systems.

Acknowledgement

This work was supported by the Post-doctoral Fellowship Program of Korea Science & Engineering Foundation (KOSEF) and by a grant from the Association for International Cancer Research (AICR).

References

1. Yeung, K., Janosch, P., Rose, D. W., Mischak, H., Sedivy, J. M., and Kolch, W.: Mechanism of Suppression of the Raf/MEK/Extracellular Signal-Regulated Kinase Pathway by the Raf Kinase Inhibitor Protein. *MOL. CELL. BIOL.* 20 (2000) 3079-3085
2. Yeung, K., Seitz, T., Li, S., Janosch, P., McFerran, B., Kaiser, C., Fee, F., Katsanakis, K. D., Rose, D. W., Mischak, H., Sedivy, J. M., and Kolch, W.: Suppression of Raf-1 kinase activity and MAP kinase signaling By RKIP. *Nature*. 401 (1999) 173-177
3. Bock, H. G.: Numerical treatment of inverse problems in chemical reaction kinetics. *Modeling of Chemical Reaction Systems*. 18 (1981) 102-125
4. Hegger, R., Kantz, H., Schmuser, F., Diestelhorst, M., Kapsch, R. P., and Beige, H.: Dynamical properties of a ferroelectric capacitor observed through nonlinear time series analysis. *Chaos*. 8 (1998) 727-736
5. Hegger, R., Kantz, H., Schmuser, F., Diestelhorst, M., Kapsch, R. P., and Beige, H.: Dynamical properties of a ferroelectric capacitor observed through nonlinear time series analysis. *Chaos*. 8 (1998) 727-736
6. Voit, E. O., *Computational Analysis of Biochemical Systems*, Cambridge University Press: Cambridge, U.K., 2000
7. Marshall, C. J., Specificity of receptor tyrosine kinase signaling: transient versus sustained extracellular signal-regulated kinase activation: *Cell*. 80 (1995) 179-185
8. Zhou, B., Wang, Z. X., Zhao, Y., Brautigan, D. L., and Zhang, Z. Y.: The specificity of extracellular signal-regulated kinase 2 dephosphorylation by protein phosphatases. *J Biol Chem*. 277 (2002) 31818-31825

Appendix: The mathematical model of ERK pathway regulated by RKIP, time course data, and estimated parameter values

The following set of nonlinear ODEs (5) represents the developed mathematical model of the ERK pathway suppressed by RKIP shown in Fig. 1.

$$\begin{aligned}
\frac{dm_1(t)}{dt} &= -k_1 m_1(t) m_2(t) + k_2 m_3(t) + k_5 m_4(t) \\
\frac{dm_2(t)}{dt} &= -k_1 m_1(t) m_2(t) + k_2 m_3(t) + k_{11} m_{11}(t) \\
\frac{dm_3(t)}{dt} &= k_1 m_1(t) m_2(t) - k_2 m_3(t) - k_3 m_3(t) m_9(t) + k_4 m_4(t) \\
\frac{dm_4(t)}{dt} &= k_3 m_3(t) m_9(t) - k_4 m_4(t) - k_5 m_4(t) \\
\frac{dm_5(t)}{dt} &= k_5 m_4(t) - k_6 m_5(t) m_7(t) + k_7 m_8(t) \\
\frac{dm_6(t)}{dt} &= k_5 m_4(t) - k_9 m_6(t) m_{10}(t) + k_{10} m_{11}(t) \\
\frac{dm_7(t)}{dt} &= -k_6 m_5(t) m_7(t) + k_7 m_8(t) + k_8 m_8(t) \\
\frac{dm_8(t)}{dt} &= k_6 m_5(t) m_7(t) - k_7 m_8(t) - k_8 m_8(t) \\
\frac{dm_9(t)}{dt} &= -k_3 m_3(t) m_9(t) + k_4 m_4(t) + k_8 m_8(t) \\
\frac{dm_{10}(t)}{dt} &= -k_9 m_6(t) m_{10}(t) + k_{10} m_{11}(t) + k_{11} m_{11}(t) \\
\frac{dm_{11}(t)}{dt} &= k_9 m_6(t) m_{10}(t) - k_{10} m_{11}(t) - k_{11} m_{11}(t)
\end{aligned} \tag{5}$$

The following Table 2 and 3 show the time course data used for parameter estimation.

Table 2. Time course data used for parameter estimation

Time \ States[μM]	m_1	m_2	m_3	m_4	m_5	m_6
t_0	120.00	48.00	1.500	4.800	12.400	4.800
t_1	67.95505535	0.3727182703	0.09086956972	58.25407508	0.08846427918	0.2285471542
t_2	66.81423242	0.05476449029	0.1696162456	59.46880595	0.044260337	0.01466380983
t_3	66.71360883	0.05019133182	0.01767995587	59.56871120	0.04176942763	0.01527704430
t_4	66.75214784	0.05490721213	0.01816772905	59.52968441	0.03971032950	0.01349091559
t_5	66.63570088	0.05405994303	0.01801622209	59.64628287	0.03590036227	0.01158526073
t_6	66.68508855	0.05314008775	0.01784579291	59.59706563	0.03603602473	0.01172030400
t_7	66.86290844	0.06026147126	0.01994358152	59.41714795	0.04015689155	0.01337477790
t_8	66.58789649	0.04974222183	0.01621135867	59.69589212	0.03435528707	0.01089921955

t_9	66.72289041	0.04488809471	0.01739192477	59.55971763	0.04010491475	0.01208455211
t_{10}	66.74940877	0.05439326527	0.01921204205	59.53137916	0.03968304675	0.01232880325

Table 3. Time course data for parameter estimation (continued)

Time \ States [μM]	m_7	m_8	m_9	m_{10}	m_{11}
t_0	87.8	3.7	240.2	160.5	2.7
t_1	70.87529418	20.62470582	182.1327548	160.1405176	3.059482367
t_2	66.32835993	25.17164007	176.4152936	160.9551958	20244804126
t_3	63.54630193	27.95369807	173.5358213	161.0518595	2.148140465
t_4	62.88014832	28.61985168	172.9107536	161.0162502	2.183749727
t_5	64.13673735	27.36326265	174.0545541	161.1299442	2.070055695
t_6	65.00392062	26.49607938	174.9708189	161.0797717	2.120228173
t_7	63.70607809	27.79392191	173.8487732	160.9107277	2.289272205
t_8	65.27236498	26.22763502	175.1421175	161.1727448	2.027255065
t_9	65.81873686	25.68126314	175.8189142	161.0340821	2.165917780
t_{10}	65.03152288	26.46847712	175.0604606	161.0173132	2.182686714

The following Table 4 and 5 summarize the estimated parameter values.

Table 4. The estimated parameter values.

Time \ Parameter	k_1	k_2	k_3	k_4	k_5	k_6
t_1	0.24	0.0048	0.38	0.0012	0.015	0.34
t_2	0.34	0.0051	0.45	0.0016	0.019	0.42
t_3	0.43	0.00678	0.51	0.0021	0.024	0.59
t_4	0.47	0.00688	0.59	0.0022	0.029	0.76
t_5	0.5	0.0071	0.62	0.0024	0.03	0.87
t_6	0.52	0.0072	0.634	0.0023	0.031	0.869
t_7	0.497	0.00701	0.621	0.00254	0.034	0.871
t_8	0.531	0.00691	0.67	0.0024	0.029	0.867
t_9	0.612	0.0073	0.65	0.0026	0.031	0.78

t_{10}	0.524	0.0075	0.61	0.00251	0.032	0.81
----------	-------	--------	------	---------	-------	------

Table 5. The estimated parameter values (continued).

Time \ Parameter	k_7	k_8	k_9	k_{10}	k_{11}
t_1	0.0013	0.02	0.37	0.00087	0.43
t_2	0.00392	0.027	0.48	0.00097	0.54
t_3	0.00487	0.0412	0.582	0.0011	0.67
t_4	0.00598	0.058	0.796	0.00118	0.789
t_5	0.0078	0.07	0.96	0.0012	0.87
t_6	0.0071	0.073	0.98	0.00125	0.869
t_7	0.0075	0.068	0.94	0.00131	0.875
t_8	0.0081	0.072	0.987	0.00118	0.867
t_9	0.0083	0.074	0.95	0.00115	0.846
t_{10}	0.007	0.069	0.961	0.00126	0.872